# Ring-Opening Metathesis Polymerization: Access to a New Class of Functionalized, Monolithic Stationary Phases for Liquid Chromatography

**ARTICLE** *in* ANGEWANDTE CHEMIE INTERNATIONAL EDITION · APRIL 2000

Impact Factor: 11.26 · DOI: 10.1002/(SICI)1521-3773(20000417)39:8<1433::AID-ANIE1433>3.0.CO;2-B



**2 AUTHORS:**

Frank Sinner
Joanneum Research Forschungsgesellschaft …
**87** PUBLICATIONS **1,906** CITATIONS
SEE PROFILE

Michael R Buchmeiser
Universität Stuttgart
**333** PUBLICATIONS **7,636** CITATIONS
SEE PROFILE

# A New Class of Continuous Polymer Supports Prepared by Ring-Opening Metathesis Polymerization: A Straightforward Route to Functionalized Monoliths

**Frank Sinner and Michael R. Buchmeiser***

*Institute of Analytical Chemistry and Radiochemistry, University of Innsbruck, Innrain 52 a, A-6020 Innsbruck, Austria*

*Received February 22, 2000; Revised Manuscript Received May 19, 2000*

ABSTRACT: Functionalized monolithic materials have been prepared by ring-opening metathesis copolymerization of norborn-2-ene (NBE) and 1,4,4a,5,8,8a-hexahydro-1,4,5,8-*exo,endo*-dimethanonaphthalene (DMN-H6) within borosilicate columns in the presence of porogenic solvents such as toluene, methylene chloride, methanol, and 2-propanol. Grubbs-type initiators of the general formula $Cl_2(PR_3)_2Ru(=CHPh)$ (R = phenyl, cyclohexyl) were used throughout. The resulting separation media possess microstructures consisting of microporous, spherical microglobules with a narrow microglobule size distribution. By variation of the polymerization conditions in terms of stoichiometry of the monomers, porogenic solvents, and temperature, microglobule diameters may be varied within a range of $2 \pm 1$ $\mu$m up to $30 \pm 10$ $\mu$m. Specific surface areas ($\sigma$) and inter-microglobule pore volumes ($\epsilon_z$) may be altered within 60−210 $m^2/g$ and 2−50%, respectively. Nonfunctionalized separation media were successfully used for the separation of 10 different model proteins using reversed phase chromatography. Generally, high flow rates of up to 10 mL/min indicating fast mass transfer may be applied, resulting in fast and efficient separations. Functionalized continuous rods were synthesized by one additional synthetic step that takes advantage of the living character of the ROMP-based copolymerization. This "in situ" derivatization was achieved after the formation of the continuous rod by reacting the active, surface-bound initiator with functional, norborn-2-ene- and 7-oxanorborn-2-ene-based monomers such as *endo,endo*-7-oxabicyclo[2.2.1]-hept-2-ene-5,6-dicarboxylic anhydride (**I**), *endo/exo*-7-oxanorborn-2-ene-5-carboxylic acid (**II**), *endo,endo-N,N*-norborn-2-ene-5,6-dicarbimid-L-valine-*m*-nitroanilide (**III**), *exo,exo-N*-phenyl-7-oxabicyclo[2.2.1]hept-2-ene-5,6-dicarbimide (**IV**), *exo,exo-N*-(4-(*N*′,*N*′-dimethylaminophenyl)-7-oxanorborn-2-ene-5,6-dicarbimide (**X**), *endo/exo*-norborn-2-ene-5-ylmethylhydroxysiloxyl-$\beta$-cyclodextrin (**XI**), and *endo/exo*-7-oxanorborn-2-ene-5-carboxyl-$\beta$-cyclodextrin (**XIII**), by passing solutions thereof in dichloromethane and DMF over the rigid rod. A $\beta$-cyclodextrin-functionalized continuous rod was successfully used for the enantioselective separation of proglumide ($\beta$-blocker).

## Introduction

Packed columns represent excellent separation media for chromatographic techniques such as HPLC, capillary liquid chromatography (CLC), and capillary electrochromatography (CEC).[1] Usually, supports with well-defined particle diameters, surface areas, and pore volumes are used. Many attempts have been made to reduce the volume of stagnant mobile phase within the pores of packed stationary phases by using nonporous particles with small diameters (1−2 $\mu$m). Despite the highly favorable properties of nonporous micropellicular supports in the rapid analysis of certain biomolecules such as proteins[2] or DNA fragments,[3,4] reduced interparticle volumes lead to higher back-pressures, which generally limits the useful minimum particle size to about 1.5 $\mu$m. As an alternative approach to packed columns, separation media with a high degree of continuity, e.g., porous disks,[5−7] stacked membranes,[8] rolled cellulose sheets,[9] or woven matrices,[10] were investigated. While separation efficiencies for small molecules are often low due to nonuniform velocities across these materials, they turned out to be excellent separation media for biopolymers as was demonstrated for example by fractionating proteins by hydrophobic interaction chromatography.[8] These preliminary efforts resulted in the development of a new type of separation media, usually referred to as monolithic columns or rigid rods[11] that have already been used successfully in standard HPLC and microseparation techniques[12−18] as well as in solid-phase extraction (SPE).[19] General advantages of such rigid rods are a lower back-pressure and an enhanced diffusional mass transfer.[20,21] This allows the analyst to run separations at comparably high flow rates of up to 15 mL/min, resulting in fast and highly efficient separations. Finally, the tideous procedures of microcolumn packing as well as the preparation of capillary end frits in CLC and CEC become superfluous.

Since the introduction of continuous beds into separation sciences by Hjertén et al.,[13,22,23] these materials have been further developed.[24−27] Organic continuous beds are based on either methacrylates or poly(styrene−divinylbenzene)[24,26−29] and are almost exclusively prepared by radical polymerization. While the resulting materials have been reported to be well defined in terms of microstructure (= size and form of microglobules that form the rod), specific surface area, and pore volume,[19,25−27,30−32] the preparation of *functionalized* monoliths is still somehow limited.[24] One synthetic protocol entails the copolymerization of the corresponding functional monomer during the synthesis of the rigid rod. Despite its simplicity, two problems have to be addressed. On one hand, a major part of the functional monomer is located at the interior of the microglobules. Since these microglobules are usually nonporous or microporous, a major part of the functional groups is

* Corresponding author. Phone: Int. code + 512-507-5184, Fax: Int. code + 512-507-2677. e-mail: michael.r.buchmeiser@uibk.ac.at.

10.1021/ma000322n CCC: $19.00 
Published on Web 07/13/2000

consequently not available in course of the separation process. On the other hand, especially the presence of polar functional groups located at the interior of the microstructure forming polymer leads to unfavorable swelling properties. An alternative approach that avoids these problems entails the copolymerization of monomers possessing active sites for postderivatization, e.g., epoxide groups or azlactone groups. Those reactive groups that are located at the surface may in fact conveniently be transformed into standard functionalities such as sulfonic acids, amines,[28,33,34] or alcohols.[35,36]

In the course of our search for more straightforward and broadly applicable synthetic routes for the preparation of functionalized polymer supports for separation sciences[37−41] as well as catalysis,[42] we already demonstrated the high versatility of ring-opening metathesis polymerization (ROMP) for these purposes. Consequently, we investigated as to which extent transition-metal-catalyzed reactions may be used for the synthesis of continuous polymeric supports.[43] In this contribution, we report on the use of ROMP for the preparation and straightforward functionalization of a new class of tailor-made continuous rods. To demonstrate the utility of this approach, a few selected applications will be presented.

## Results and Discussion

**Polymerization System.** In contrast to temperature-induced radical polymerization, ROMP represents a metal-catalyzed polymerization system. In principle, Schrock and Grubbs systems, both highly active in the ROMP of strained functionalized olefins, may be applied. Since the preparation and in particular derivatization of ROMP-based rigid rods require some handling that may not be performed under strict inert atmosphere, we focused on the use of the less oxygen-sensitive ruthenium-based Grubbs-type initiators of the general formula $Cl_2(PR_3)_2Ru(=CHPh)$ (R = phenyl, cyclohexyl) rather than on the use of the molybdenum-based Schrock-type initiators $(Mo(NAr')(CHCMe_2Ph)(OR')_2)$. In a first step, a polymerization system in terms of initiator, monomer, cross-linker, and porogens for the preparation of nonfunctionalized continuous rods had to be elaborated. Generally speaking, polymerization activities of $Cl_2(PPh_3)_2Ru(=CHPh)$ with all monomers and cross-linkers investigated were found to be too low. Only gel-like structures with a low degree of cross-linking were obtained. Nevertheless, $Cl_2(PCy_3)_2Ru(=CHPh)$ (Cy = cyclohexyl **1**) turned out to be active enough and promising microstructures were obtained. Consequently, **1** was chosen as the initiator for the further preparation of monoliths. In terms of monomers, norbornene (NBE) and *exo,endo*-1,4,4a,5,8,8a-hexahydro-1,4,5,8-*exo,endo*-dimethanonaphthalene (DMN-H6) as a cross-linker were found suitable. While other monomers and cross-linkers such as norbornadiene and 1,4a,5,8,8a,9,9a,10,10a-decahydro-1,4,5,8,9,10-trimethanoanthracene turned out to be too reactive or gave rise to unfavorable microstructures, dicyclopentadiene (DCPD) did not exhibit the desired cross-linking properties. This is in accordance with previous studies, where cross-linking of DCPD was found to occur only thermally induced at high monomer concentrations.[44−46] On the basis of the existing knowledge about pore formation in monolithic materials,[19,26,32,47] different mixtures of macro- and microporogens[24] were tested for their ability to form the desired, well-defined microstructures. Generally, two solutions were prepared that contained all necessary reactants for polymer synthesis. Solution A consisted of NBE, the cross-linker, and the macroporogen; solution B consisted of the initiator and the microporogen. Both solutions were cooled to the appropriate polymerization temperature ($T_p$, see Table 1) and mixed for a few seconds before being transferred into the prechilled HPLC column. Methanol, 2-propanol, cyclohexanol, 1-decanol, and 1-dodecanol were investigated for their macropore-forming properties; dichloroethane, dichloromethane, and toluene were used as microporogens. Since THF and dimethyl sulfoxide are coordinating solvents that may reduce initiator reactivity, their use was avoided. While methanol turned out to be a poor solvent for NBE, the use of cyclohexanol, 1-decanol, and 1-dodecanol only resulted in the formation of gel-like structures. Nevertheless, 2-propanol was found to possess good macropore-forming properties. Toluene, dichloromethane, and dichloroethane were found to be capable of forming the desired microstructures in combination with 2-propanol. To avoid bubble formation due to local overheating during polymerization, toluene was used as a microporogen for all further experiments. Figure 1 gives an illustration of the microstructure, the backbone, and the relevant abbreviations.

**Monomer Ratios and Polymerization Conditions.** To investigate the influence of the relative ratios of NBE + DMN-H6 to porogens on the polymerization systems, two series of monoliths were prepared. Structural data were obtained by means of electron microscopy (ELMI) and by inverse size exclusion chromatography.[48] For all monoliths (1−13), a weight ratio of 1:1 for NBE to DMN-H6 (corresponding to a molar ratio of 6:4) was chosen. In a first series (monoliths 1−8, Table 1) the toluene content of the polymerization mixtures was kept constant at 10 wt %. As expected, the volume fraction of the inter-microglobule volume ($\epsilon_z$) constantly decreased due to the increasing NBE and DMN-H6 content. Plots of pressure vs the flow rate recorded for monoliths 1−3, 5, and 7 illustrate these changes in $\epsilon_z$. Thus, with increasing microglobule diameters and decreasing inter-microglobule volume $\epsilon_z$, higher slopes in the pressure vs flow rate diagram are obtained (Figure 2). The linearity of these plots clearly demonstrates the incompressibility of the continuous rods by the mobile phase even at high flow rates of 8 mL/min.

Interestingly, the pore volume ($V_p$) as well as the specific surface ($\sigma$) basically remained constant down to an 2-PrOH concentration of 30%. At this point, $\sigma$ increased drastically (191 $m^2/g$). This value was found to be reproducible within three independent experiments ($n = 3$, relative standard deviation $s_{n-1} = 16\%$). Similarly, the microglobule size ($d_p$) also remained constant down to a 2-PrOH concentration of 30%. In terms of morphology, no significant changes in terms of microglobule shape were observed. Obviously, the increasing monomer + cross-linker content compensates for the decreasing 2-PrOH concentration in terms of phase separation, which may at 0 °C typically be observed after approximately 2 min with systems described in Table 1. Briefly, the gelling point was determined independently by visual observation and GPC. For GPC measurements, aliquots of the polymerization mixture were withdrawn and terminated by addition of a 1:1 mixture of 1-hexene and acetonitrile. It is worth noting that the values for $M_w$ of the soluble

**Table 1. Physicochemical Data for Monoliths 1–28**[a]

| no. | NBE [%][a] | DMN-H6 [%][a] | toluene [%][a] | 2-PrOH [%][a] | **1** [%][a] | $T_p$ [°C] | $\sigma$ [m²/g] | $\sigma_c$ [m²] | $\epsilon_p$ [%] | $\epsilon_z$ [%] | $\epsilon_t$ [%] | $\rho_p$ [g/cm³] | $V_p$ [mL] | $d_p$ [$\mu$m] | microglobule shape |
|---|---|---|---|---|---|---|---|---|---|---|---|---|---|---|---|
| 1 | 15 | 15 | 10 | 60 | 0.4 | 0 | 76 | 14 | 43 | 37 | 80 | 0.27 | 0.31 | 2 ± 1 | s/a |
| 2 | 20 | 20 | 10 | 50 | 0.4 | 0 | 62 | 13 | 43 | 33 | 76 | 0.31 | 0.31 | 4 ± 1 | s |
| 3 | 25 | 25 | 10 | 40 | 0.4 | 0 | 85 | 24 | 48 | 15 | 63 | 0.40 | 0.34 | 2 ± 1 | s |
| 4 | 25 | 25 | 10 | 40 | 1 | 0 | 86 | 25 | 48 | 14 | 63 | 0.40 | 0.34 | 4 ± 1 | s |
| 5 | 30 | 30 | 10 | 30 | 0.4 | 0 | 191 | 67 | 50 | 5 | 54 | 0.46 | 0.35 | 8 ± 2 | s/a |
| 6 | 30 | 30 | 10 | 30 | 1 | 0 | 96 | 31 | 50 | 2 | 53 | 0.46 | 0.36 | 6 ± 2 | s |
| 7 | 35 | 35 | 10 | 20 | 0.4 | 0 | *b* | *b* | *b* | *b* | *b* | *b* | *b* | 14 ± 6 | a |
| 8 | 35 | 35 | 10 | 20 | 1 | 0 | *b* | *b* | *b* | *b* | *b* | *b* | *b* | *b* | *b* |
| 9 | 15 | 15 | 20 | 50 | 0.4 | 0 | 110 | 20 | 39 | 49 | 89 | 0.25 | 0.28 | 3 ± 1 | s |
| 10 | 20 | 20 | 20 | 40 | 0.4 | 0 | 74 | 19 | 44 | 21 | 65 | 0.36 | 0.31 | 4 ± 1 | s |
| 11 | 25 | 25 | 20 | 30 | 0.4 | 0 | 91 | 26 | 47 | 15 | 62 | 0.42 | 0.33 | 4 ± 1 | s |
| 12 | 30 | 30 | 20 | 20 | 0.4 | 0 | 93 | 33 | 65 | 5 | 69 | 0.50 | 0.46 | 4 ± 1 | s |
| 13 | 35 | 35 | 20 | 10 | 0.4 | 0 | *b* | *b* | *b* | *b* | *b* | *b* | *b* | 30 ± 10 | s |
| 14 | 0 | 50 | 10 | 40 | 0.4 | 0 | 88 | 20 | 44 | 25 | 69 | 0.32 | 0.31 | 2 ± 1 | s |
| 15 | 15 | 35 | 10 | 40 | 0.4 | 0 | 76 | 19 | 45 | 26 | 71 | 0.35 | 0.32 | 4 ± 1 | s |
| 16 | 25 | 25 | 10 | 40 | 0.4 | 0 | 85 | 24 | 48 | 15 | 63 | 0.40 | 0.34 | 2 ± 1 | s |
| 17 | 35 | 15 | 10 | 40 | 0.4 | 0 | 100 | 29 | 45 | 10 | 56 | 0.41 | 0.32 | 3 ± 1 | s/a |
| 18 | 25 | 25 | 10 | 40 | 0.01 | 0 | *b* | *b* | *b* | *b* | *b* | *b* | *b* | 6 ± 4 | a |
| 19 | 25 | 25 | 10 | 40 | 0.1 | 0 | 83 | 21 | 49 | 20 | 69 | 0.36 | 0.35 | 2 ± 1 | a |
| 20 | 25 | 25 | 10 | 40 | 0.4 | 0 | 85 | 24 | 48 | 15 | 63 | 0.40 | 0.34 | 2 ± 1 | s |
| 21 | 25 | 25 | 10 | 40 | 1 | 0 | 75 | 22 | 49 | 12 | 61 | 0.41 | 0.35 | 3 ± 1 | s |
| 22 | 25 | 25 | 10 | 40 | 0.4 | −30 | 97 | 27 | 50 | 13 | 63 | 0.39 | 0.35 | 8 ± 2 | s/a |
| 23 | 25 | 25 | 10 | 40 | 0.4 | −20 | 98 | 27 | 45 | 17 | 62 | 0.38 | 0.32 | 6 ± 2 | s/a |
| 24 | 25 | 25 | 10 | 40 | 0.4 | −10 | 85 | 24 | 47 | 10 | 58 | 0.39 | 0.33 | 4 ± 2 | s |
| 25 | 25 | 25 | 10 | 40 | 0.4 | 0 | 85 | 24 | 48 | 14 | 63 | 0.40 | 0.34 | 2 ± 1 | s/a |
| 26 | 25 | 25 | 10 | 40 | 0.4 | 25 | *c* | *c* | *c* | *c* | *c* | *c* | *c* | 3 ± 1 | s/a |
| 27 | 25 | 25 | 10 | 40 | 0.4 | 60 | *c* | *c* | *c* | *c* | *c* | *c* | *c* | 2 ± 1 | s/a |
| 28 | 25 | 25 | 10 | 40 | 0.4 | 90 | *c* | *c* | *c* | *c* | *c* | *c* | *c* | 2 ± 1 | s/a |

[a] NBE = norborn-2-ene, DMN-H6 = 1,4,4a,5,8,8a-hexahydro-1,4,5,8-*exo*,*endo*-dimethanonaphthalene, **1** = initiator, $T_p$ = polymerization temperature, $\sigma$ = specific surface, $\sigma_c$ = total surface area of monolith, $\epsilon_p$ = volume fraction of pores,[66] $\epsilon_z$ = volume fraction of inter-microglobule void volume,[66] $\epsilon_t$ = volume fraction occupied by mobile phase,[66] $\rho_p$ = apparent density,[66] $V_p$ = pore volume,[66] $d_p$ = microglobule diameter,[66] s = spherical, a = agglomerated. [b] Not analyzed by GPC due to high back-pressure. [c] Incomplete attachment to inner wall due to polymerization conditions. [d] By weight.

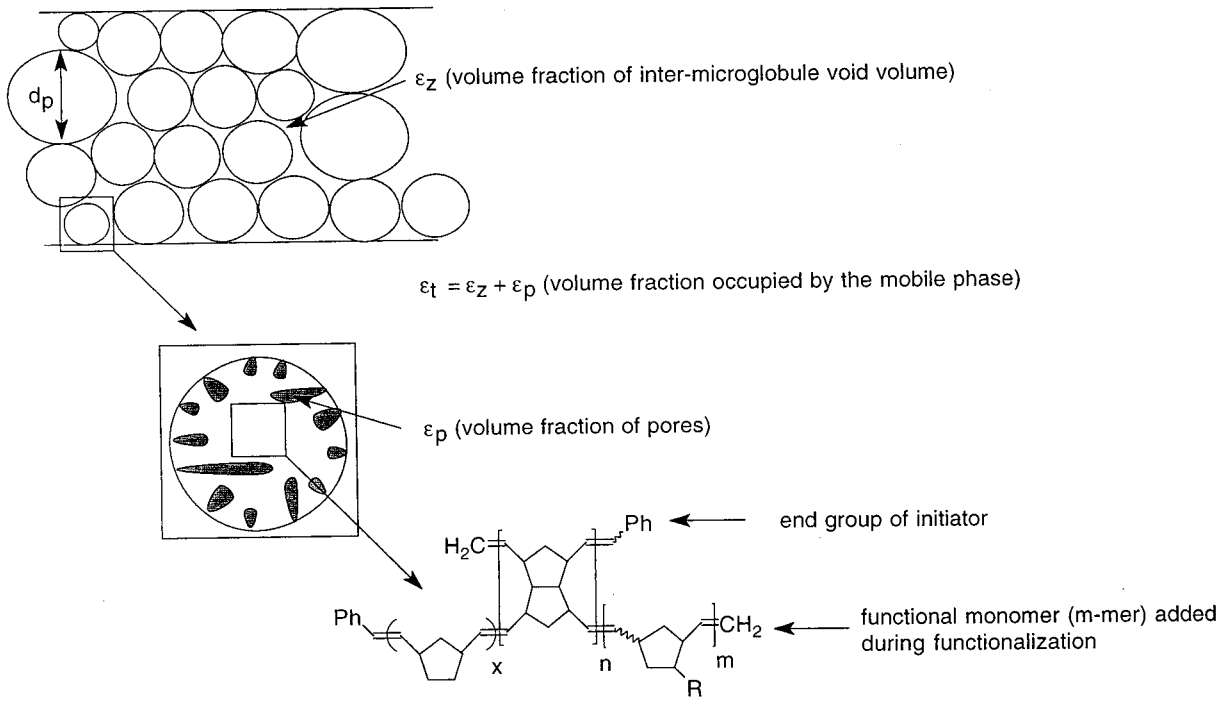


**Figure 1.** Illustration of the physical meanings of $d_p$, $\epsilon_z$, $\epsilon_p$, and $\epsilon_t$ and schematic drawing of the backbone structure. R = functional group.

fraction at the gelling point did not exceed 15 000 Da, indicating a high degree of cross-linking. Finally, lowering the 2-PrOH concentration down to 20% led to an increase in $d_p$ of up to 14 $\mu$m. Since in radical vinyl polymerization large microglobules are usually formed by an early stage phase separation at *low* monomer conversions followed by diffusion of residual monomer into the growing nuclei,[27,30,49] one needs to address this "reverse" behavior. Thus, phase separation and rod formation proceed slowly in thermally induced radical

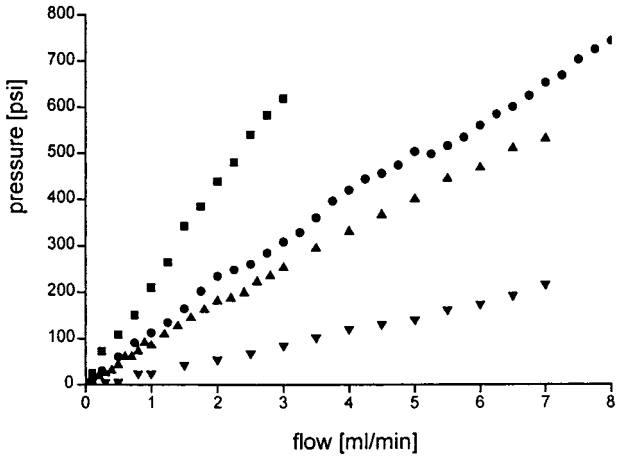


**Figure 2.** Flow vs back-pressure plots recorded for monoliths 1 (▼), 2 (▲), 3 (●), and 5 (■). Chromatographic conditions: column 3 × 50 mm i.d., room temperature, mobile phase, water. For polymerization conditions refer to Experimental Section.

polymerizations compared to transition-metal-catalyzed polymerizations. We therefore attribute the formation of the larger microglobules in the present system to a type of delayed phase separation where the continuous rod splits into a few, large microglobules at *high* monomer conversions. This is supported by the finding that transparent, filmlike, "nonseparated" structures were obtained with a 2-PrOH content of 20% or less.

In a second series (entries 9−13), the toluene content was raised to 20 wt %, again using a 1:1 ratio of NBE to DMN-H6. As can be deduced from Table 1, the same changes in $d_p$, $\epsilon_z$, $\sigma$, and $V_p$ were observed. Because of the increase in the toluene concentration, a delayed phase separation was observed again. Consequently, large microglobule formation only occurred at 2-PrOH concentrations of 10%. At concentrations of NBE plus DMN-H6 (entry 13) of larger than 70% (35% + 35%), phase separation did no longer occur, and polymeric films were obtained.

To investigate the influences of the NBE to DMN-H6 ratio onto the microstructure, monoliths 14−17 were synthesized (Table 1). Variations of NBE to DMN-H6 ratios revealed no significant changes in $d_p$ and $\epsilon_z$ as well as in $\sigma$. Thus, all monoliths possessed microglobule diameters of 2−4 $\mu$m with surface areas in the range 80−100 $m^2/g$. No influence of the NBE to DMN-H6 ratio onto the homogeneity of the microstructure was found. Since the system 10% toluene−40% 2-PrOH appeared to be "stable" in terms of morphology and small deviations in composition did not result in a dramatic change in morphology, it was used as a basis for the synthesis of functionalized monoliths (vide infra).

**Initiator Concentration.** Initiator concentrations represent a crucial point in the preparation of monoliths. On one hand, any uncontrolled, highly exothermic reaction must be strictly avoided. On the other hand, the total amount of initiator directly determines the amount of growing nuclei that are responsible for phase separation and microglobule size. Nevertheless, in terms of a desired in situ derivatization, higher initiator concentrations are generally highly favorable. Since the initiator is distributed homogeneously within the rod, only a small fraction of the initiator located at the surface of the rod-forming microglobuls may be used for derivatization. Consequently, only high initiator concentrations guarantee a sufficient surface derivatization. To determine the scopes and limitations of **1**, initiator concentrations were varied over a range of 2 orders of magnitude (0.01−1%). Besides some effects on the microglobule shape, no significant influences on the morphology in terms of pore and microglobule size of the continuous rods were observed. While small amounts of initiator (0.01%, entry 18; 0.1%, entry 19) result in microstructures with larger microglobules, larger amounts of **1** lead to microstructures that consist of smaller microglobules (entries 20 and 21). Since rods prepared with low amounts of initiator turned out to be compressible (e.g., entry 18), 1−2% of **1** were used for rod formation and found to be sufficient for derivatization purposes without changing the properties of the rods in terms of microstructure.

At this point, when dealing with transition-metal-catalyzed polymerizations, the efficiency of removing the metal from the rod after polymerization needs to be addressed. While ruthenium-initiated polymerizations may conveniently be capped with 1-hexene, we found the use of acetonitrile even more favorable. Thus, addition of acetonitrile to any ruthenium-based polymerization system leads to an instantaneous termination, presumably via metathesis of the nitrile group. In contrast to standard termination systems, the resulting Ru species is obviously stabilized by the excess of acetonitrile ligands, which allows its efficient removal. ICP-OES investigations on the Ru content of the rods revealed Ru concentrations <10 $\mu$g/g.

**Temperature.** Pore properties and microstructures of bulk polymers are directly related to phase separation phenomena that are in turn affected by temperature. In *radical* polymerizations, temperature additionally influences the morphology of the resulting monoliths since it also determines the total amount of free radicals and consequently the number of growing nuclei.[30] Since these nuclei grow to the form of globules, higher initiator concentrations translate into a larger amount of globules that are consequently smaller in size. Transition-metal-catalyzed, "living" polymerizations differ in that the total amount of growing polymer chains remains independent of polymerization temperature ($T_p$) if initiation is quantitative. Since initiations by **1** are often found to be nonquantitative in terms of initiator consumption,[39,40] an influence of $T_p$ had to be expected. To elucidate the present polymerization system, a series of monoliths (entries 22−28) were prepared at temperatures varying from −30 up to 90 °C. As can be deduced from Table 1, microglobule diameters were strongly affected by $T_p$. Thus, increasing the polymerization temperature from −30 to 90 °C results in the formation of smaller microglobules. Microglobule shape was found to remain unaffected by this increase in $T_p$. These findings may now be explained by the influence of polymerization temperature on initiator efficiency. Thus, low polymerization temperatures (−30 °C) *decrease* the efficiency of **1**. This leads to a reduced amount of growing nuclei, resulting in the formation of larger microglobules. On the other hand, elevated temperatures increase initiator activity and lead to the formation of a larger amount of growing nuclei and consequently to the formation of smaller microglobules. Additionally, phase separation is delayed at higher $T_p$ values due to the enhanced solubility of the polymers in the system.

In summary, by choosing adequate polymerization mixtures and conditions, continuous rods with designed,

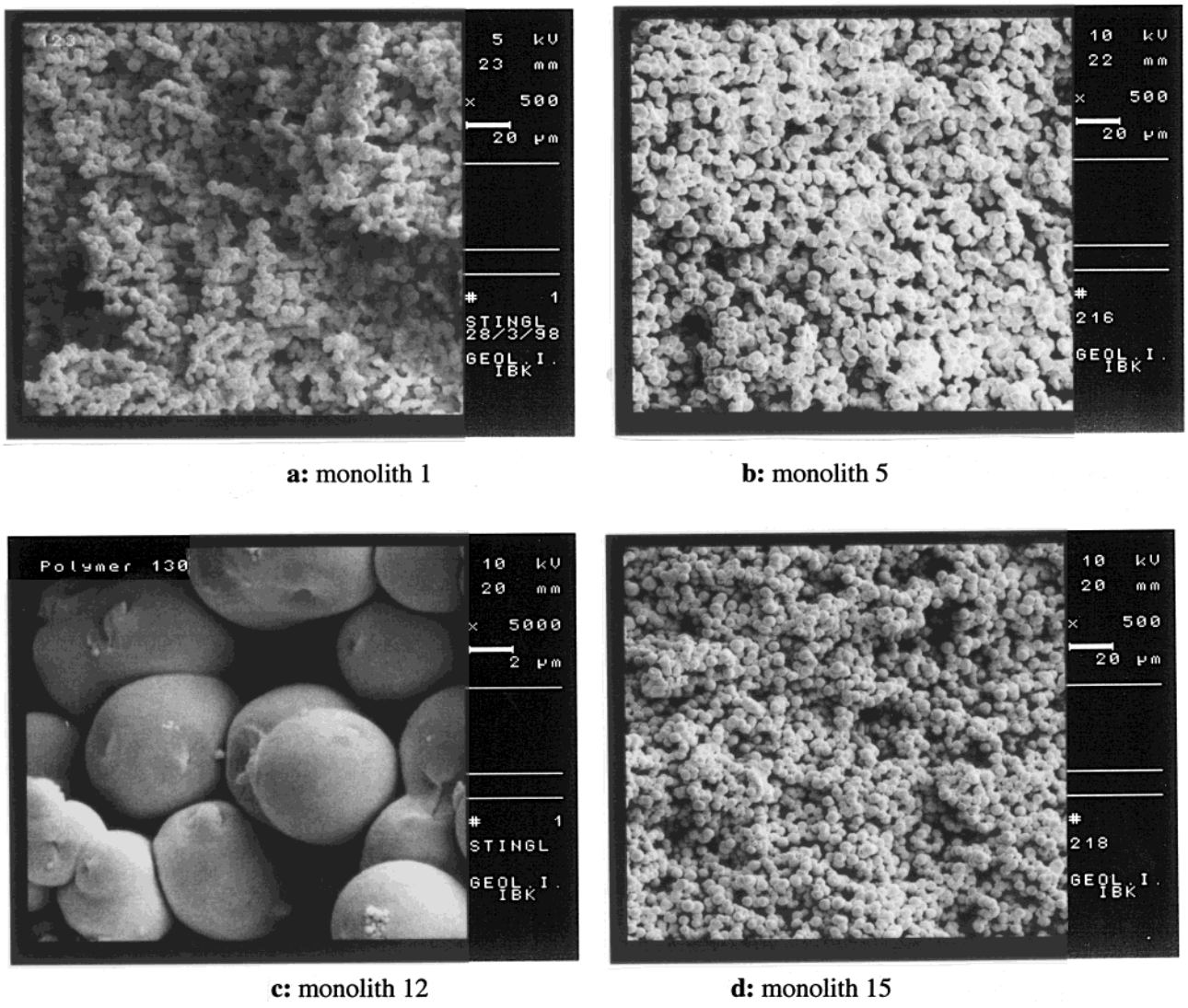


**Figure 3.** Electron microscope pictures of monoliths 1, 5, 12, and 15.

homogeneous microstructures in terms of microglobule and inter-microglobule void volume may be prepared. Representative ELMI pictures that show the microstructures of such monoliths are shown in Figure 3a–d.

**Shrinkage.** Shrinkage is an unavoidable process in any vinyl polymerization[50] and leads to longitudinal and radial contraction of the so-formed, rodlike polymer. Despite the comparably low shrinkage of poly-NBE-based systems (<5%), all polymers formed by in-column polymerization of NBE and DMN-H6 by **1** in the presence of any of the examined porogens exhibit longitudinal and radial shrinkage. Shrinkage, which usually leads to a detachment of the continuous bed from the inner column wall, may not be suppressed by changing the porogen-to-monomer ratio or by varying the cross-linker-to-monomer ratio. Consequently, covalent fixation of the polymer rod to the inner wall of the mold via anchor groups is necessary. This may be achieved by silanization of the activated inner glass wall with bicyclo[2.2.1]hept-2-ene-5-trichlorosilane, leading to the presence of ROMP-active norbornene anchor groups. These anchor groups become copolymerized during the continuous rod formation. While the use of anchor groups eliminates radial shrinkage, longitudinal shrinkage at the column ends still occurs. Nevertheless, this longitudinal shrinkage may be compensated by using an adequate polymerization arrangement as shown in Figure 4. Using this arrangement, longitudinal shrinkage takes place outside the confines of the mold, and a perfectly filled HPLC column is obtained.

**Functionalization of Monoliths.** For reasons already briefly outlined at the beginning, an in situ functionalization that allows the use of *any* functional group seemed highly favorable. For these purposes, we took advantage of the "living" character[51−54] of many ruthenium-based metathesis polymerizations and their high tolerance vs different functionalities. While a grafting approach on TEMPO-capped monoliths has been proposed recently,[55] the ROMP approach is believed to be more attractive in terms of functional variety. Since any living polymerization system is not immortal[56,57] and in view of the stability data for ruthenium-based initiators and in particular for **1**,[58] optimum grafting conditions were elaborated in order to reduce loss of initiator activity to a minimum. For these purposes, the minimum time needed for the formation of the polymeric backbone was determined. Three identical monoliths (entry 5) were prepared, and polymerization was terminated after 30, 60, and 90 min by pumping 1-hexene/toluene through the columns to wash out unreacted monomers. Few unreacted cross-linker or norbornene (monomer conversion > 95%) was detected after 60 min, indicating that matrix formation

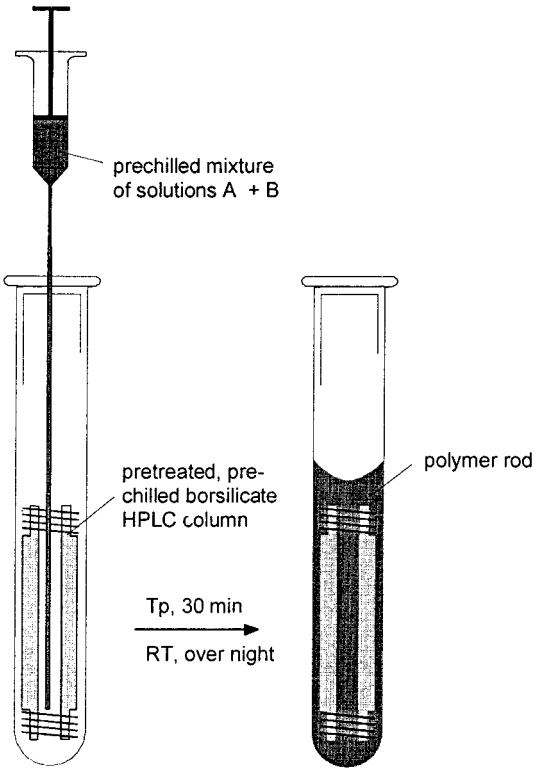


**Figure 4.** Polymerization arrangement for the preparation of molded continuous rods using ROMP.

was completed after this time. As a compromise between the total conversion of NBE and DMN-H6 and the shortest time period needed for structure formation, 1 h was chosen between initiation and "in situ" derivatization. At this stage major amounts of the catalyst are still active. Using the fraction of the initiator covalently bound to the surface, the desired functional monomer is grafted onto the monolith surface by simply passing a solution thereof through the column. This approach offers multiple advantages. First, the structure of the continuous rod is not influenced by the functional monomer and can be optimized regardless of the functional monomer used. Second, other solvents than the porogens toluene and methanol (e.g., methylene chloride, DMF) may be used for the "in situ" derivatization of the rod. This avoids possible limitations related to the solubility of the functional monomer in the porogens (e.g., $\beta$-cyclodextrins are only soluble in DMF). Finally, a large variety of functional monomers may be grafted onto the continuous rod. Restrictions due to a reduced polymerization activity of **1** vs a functional monomer may be avoided by a careful monomer design. To demonstrate the versatility of this concept, different functionalized monoliths (monoliths 5D−5I, 6J, 6K) bearing different functionalities were prepared. Table 2 summarizes data from different functionalized continuous rods. Generally, all functional monomers employed were either based on norborn-2-ene or 7-oxanorborn-2-ene (Figure 5). The amount of functional monomer grafted onto the monolith was determined by elemental analysis and titration, respectively.

As can be deduced from Table 2, capacities (expressed in mmol of functional monomer/g) of 0.03−0.3 mmol/g have been obtained. Except for monoliths 4F and 6J, this extent of functionalization was found to be sufficiently high for chromatographic applications (vide infra).

**Table 2. Capacities of Functionalized ROMP Monoliths**

| monolith | monomer | capacity [mmol/g] (amount of functional monomer [wt %]) |
|---|---|---|
| 4D | **I** | 0.2[a] (3.3) |
| 4E | **II** | 0.14[a] (2.0) |
| 4F | **III** | 0.03[b] (1.1) |
| 4G | **IV** | 0.22[b] (5.3) |
| 4H | **VII** | 0.06[b] (1.5) |
| 4I | **X** | 0.26[b] (7.4) |
| 6J | **XI** | 0.001[c] (0.1) |
| 6K | **XIII** | 0.003[c] (0.4) |

[a] Determined by titration. [b] Determined by elemental analysis (percent of nitrogen). [c] Estimated by comparison with loading capacities and structural data of surface-grafted materials.[40]

**Chromatographic Properties.** Monoliths prepared from NBE and DMN-H6 are strongly hydrophobic. Nevertheless, the resulting materials significantly differ from PS-DVB-based resins, in that the latter one contains aromatic systems that are capable of forming $\pi$-stacks with analytes possessing aromatic groups. Figure 6 shows the fast separation of 10 different biologically relevant proteins by reversed phase chromatography. At flow rates of 2 mL/min, this separation may be accomplished within 3 min. This separation performance at high flow rates gives an illustration of the fast mass transfer that may be achieved.

To demonstrate the applicability of the in situ derivatization concept, monolith 6J, bearing norborn-2-ene-5-ylmethylhydroxysiloxyl-$\beta$-cyclodextrin (**XI**) as a chiral selector, was used for enantioselective separations. Low enantiomeric separation performance ($R_s$ < 0.5) was observed and may be attributed to a low capacity of **XI**, a direct result of the low polymerization activity of **1** vs the chiral selector.[40] Since ruthenium-based initiators exhibit high polymerization activity vs 7-oxanorbornene-based monomers, monolith 6K was derivatized with 7-oxanorborn-2-ene-5-carboxyl-$\beta$-cyclodextrin (**XIII**). As expected, higher cyclodextrin loadings were obtained, and separation of D- and L-proglumide ($R_s$ = 1.05, $\alpha$ = 1.39) was achieved under the same chromatographic conditions as used for monolith 6J (Figure 7).

## Conclusions

A new class of continuous rods prepared by ROMP of norbornene and 1,4,4a,5,8,8a-hexahydro-1,4,5,8-*exo,endo*-dimethanonaphthalene has been presented. The materials are characterized by highly regular polymer microstructures adjustable between 2−30 $\mu$m, a narrow microglobule size distribution, and excellent chromatographic properties. Furthermore, a new straightforward concept for the preparation of functionalized continuous rods was elaborated. In this context, functionalization was achieved by an additional in situ derivatization step taking advantage of the living manner of this type of polymerization. A large variety of functionalized continuous rods were prepared, and their applicability in chromatographic science was demonstrated by the enantioselective separation of proglumide on a $\beta$-cyclodextrin functionalized continuous rod. We are currently extending this synthetic approach to the synthesis of functionalized monoliths for microapplications such as CLC as well as for applications in heterogeneous catalysis.

## Experimental Section

**Instrumentation.** NMR data were obtained in the indicated solvent at 25 °C on a Bruker Spectrospin 300 and are

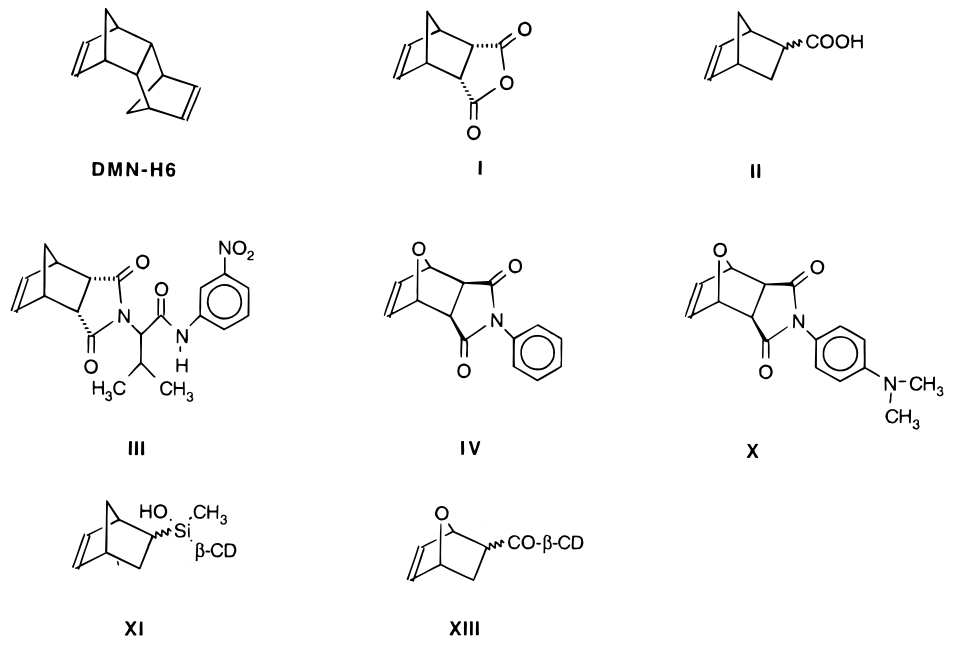


**Figure 5.** Structures of compounds DMN-H6, **I**−**IV**, **X**, **XI**, and **XIII**.

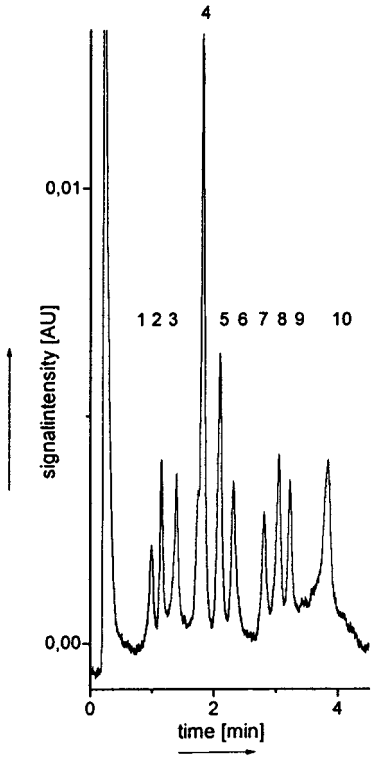


**Figure 6.** Protein separation. Mobile phase A: acetonitrile + 0.1% TFA; mobile phase B: water + 0.1% TFA on monolith 3. Gradient: 0−0.5 min 21−36% B. 36−40% B within 2 min, up to 55% B in 0.5 min; flow: 2 mL/min, injection volume: 4 $\mu$L (20 $\mu$g/mL each), UV (218 nm). Analytes: (1) ribonuclease A, (2) insulin, (3) cytochrome C, (4) lysozyme, (5) $\beta$-lactoglobulin A, (6) transferrin, (7) myoglobin, (8) α-chymotrypsinogen A, (9) catalase, (10) ovalbumin.

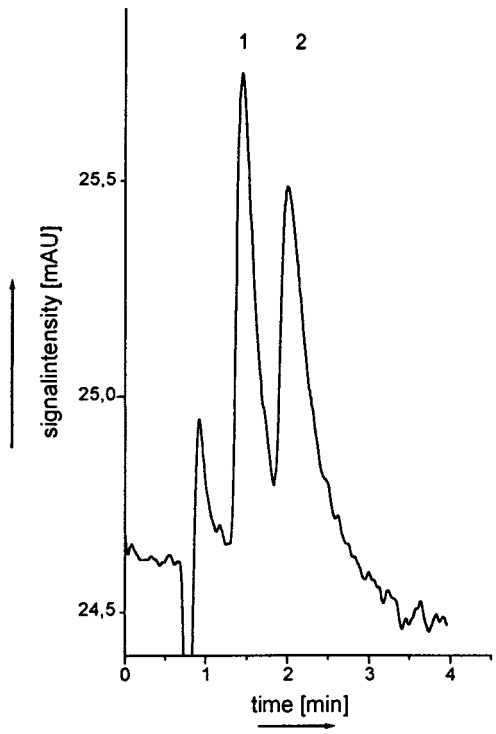


**Figure 7.** Chiral separation of proglumide on monolith 6K. Mobile phase: 99.75/0.25/0.025/0.075 ACN/MeOH/TFA/TEA (v/v/v/v), $T$ = 0 °C, flow: 2 mL/min); injection volume: 4 $\mu$L (20 $\mu$g/mL), UV (254 nm).

listed in parts per million downfield from tetramethylsilane for proton and carbon. Coupling constants are listed in hertz. IR spectra were recorded on a Nicolet 510 FT-IR. Titrations were performed using a 686 Titroprocessor (Metrohm, Switzerland). HPLC experiments were carried out on a Waters LC-module 1 plus (UV detector) and on a Waters 600 S controller system (484 UV detector), using a Baseline work package (Waters). Eluents were degasses with He 5.0. Elemental analyses were carried out at the Institute of Physical Chemistry, University of Vienna. Further instrumentation for ICP-OES experiments and for the determination of the specific surface area ($\sigma$) by means of GPC is described elsewhere.[41]

**Reagents and Standards.** All experiments were performed under an argon atmosphere by standard Schlenk techniques or in an Ar-mediated drybox (Braun, Germany) unless stated otherwise. Reagent grade diethyl ether, pentane, tetrahydrofuran, and toluene were distilled from sodium benzophenone ketyl under argon. Reagent grade dichloromethane, methanol, 2-propanol, ethanol, 1,2-dichloroethane, and pyridine were distilled from calcium hydride under argon. Dicyclopentadiene (DCP), bicyclo[2.2.1]hept-2,5-diene, 1-de-

canol, 1-dodecanol, and cyclohexanol were distilled and stored over molecular sieves under argon. *N*,*N*-Dimethylformamide (DMF) was dried over molecular sieves. Deionized water was used throughout. *endo*,*endo*-7-Oxabicyclo[2.2.1]hept-2-ene-5,6-dicarboxylic anhydride (**I**),[59,60] poly(**1**),[61] *endo*-norborn-2-ene-5-carboxylic acid chloride,[41] 7-oxanorborn-2-ene-5-carboxylic acid (**II**),[62] *endo*,*endo*-*N*,*N*-norborn-2-ene-5,6-dicarbimid-L-valine-*m*-nitroanilide (**III**),[40] *exo*,*exo*-*N*-phenyl-7-oxabicyclo-[2.2.1]hept-2-ene-5,6-dicarbimide (**IV**),[63] 1,4,4a,5,8,8a-hexahydro-1,4,5,8-*exo*,*endo*-dimethanonaphthalene (DMN-H6), 1,-4a,5,8,8a,9,9a,10,10a-decahydro-1,4,5,8,9,10-trimethanoanthracene (CL-2),[64] and the initiators $Cl_2(PR_3)_2Ru(=CHPh)$ (R = phenyl, **2**, R = cyclohexyl **1**)[65] were prepared according to literature procedures and checked for purity by means of NMR. A full characterization of poly-**I**[61] and poly-**III**[40] prepared by Ru-based initiators is given elsewhere. Proglumide was purchased from Sigma (Vienna, Austria). Norborn-2-ene, bicyclo-[2.2.1]hept-2,5-diene, dicyclopentadiene (DCP), *N*,*N*-dimethylformamide (DMF), aniline, acetic acid anhydride, 4-aminophenol, dicyclohexylcarbodiimide, 4-amino-*N*,*N*-dimethylaniline, sodium acetate anhydrous, sodium hydrogen carbonate, *β*-cyclodextrin, maleic anhydride, triethylamine (TEA), trifluoroacetic acid (TFA), and deuterated solvents were purchased from Fluka (Buchs, Switzerland). Bicyclo[2.2.1]hept-2-ene-5-yltrichlorosilane and bicyclo[2.2.1]hept-2-ene-5-ylmethyldichlorosilane were purchased from ABCR (Darmstadt, Germany). Acryloyl chloride, furan, and 1-decanol were purchased from Merck (Darmstadt, Germany).

***N*-(4-Hydroxyphenyl)maleic Monoanilide (V).** Maleic anhydride (10.0 g, 0.10 mol) was dissolved in diethyl ether, and 4-aminophenol (11.0 g, 0.1 mol) was added. The solution was refluxed for 16 h. The yellow precipitate was filtered off, washed with cold diethyl ether, and dried in vacuo. Yield: 19.8 g (95.6%). IR (KBr, $cm^{-1}$): 3670 m, 3200 bs, 1700 w, 1690 s, 1625 w, 1620 s, 1240 w, 1225 w, 1180 m, 1070 m, 840 s, 810 s, 715 bm, 715 bm. $^1$H NMR (DMSO-$d_6$): $\delta$ 10.4 (s, 1 H, OH), 9.35 (s, 1 H, NH), 7.43, (d, 2 H, $J$ = 6.8), 6.74 (d, 2 H, $J$ = 6.8), 6. 47 (d, 1 H, $J$ = 12.1, C*H*=CH), 6. 28 (d, 1 H, $J$ = 12.1, CH=C*H*), 3.48 (s, 1 H, OH). $^{13}$C NMR (DMSO-$d_6$): $\delta$ 166.3 (*C*O), 162.7 (*C*O), 154.1, 131.7, 131.2, 129.7, 121.5 (*C*=C), 115.2 (C=*C*). Elemental analysis: Calcd for $C_{10}H_9NO_4$ ($M_w$ = 207.18): C, 57.97; H, 4.38; N, 6.76. Found: C, 57.75; H, 4.36; N, 6.60.

***N*-(4-Hydroxyphenyl)maleimide (VI).** A solution of *N*-(4-hydroxyphenyl)maleic monoanilide (19.8 g, 103 mmol) and dicyclohexylcarbodiimide (20 g, 97 mmol) in dichloromethane was refluxed for 18 h. The precipitate was filtered off, washed with cold dichloromethane, and dissolved in acetonitrile. Urea was filtered off, and acetonitrile was evaporated under reduced pressure. Yield: 14.3 g (78%). IR (KBr, $cm^{-1}$): 3350 m, 3180 bs, 3060 s, 3020 w, 2890 m, 1760 s, 1670 s, 1630 w, 1580 s, 1235 s, 1225 s, 805 m, 790 s, 730 vs. $^1$H NMR ($D_3$CCN): $\delta$ 7.22 (s, broad, 1H, $H_5$), 7.12 (m, 2H, $H_{3,7}$), 6.88 (m, 4H, $H_{1,2,4,6}$). $^{13}$C NMR ($D_3$CCN): $\delta$ 171.4 ($C_{1,4}$), 157.7 ($C_8$), 135.4 ($C_{2,3}$), 129.5 ($C_{6,10}$), 124.7 ($C_5$), 116.6 ($C_{7,9}$). Elemental analysis: Calcd for $C_{10}H_7NO_3$ ($M_w$ = 189.17): C, 63.49; H, 3.73; N, 7.40. Found: C, 63.19; H, 3.87; N, 7.27.

***exo*,*exo*-*N*-4-Hydroxyphenyl-7-oxabicyclo[2.2.1]hept-2-ene-5,6-dicarbimide (VII).** *N*-(4-Hydroxyphenyl)maleimide (3.0 g, 16 mmol) was dissolved in diethyl ether, and furan (9.4 g, 138 mmol) was added. The solution was heated to 130 °C for 18 h and cooled to 0 °C, and the precipitate was filtered off. The precipitate was washed with diethyl ether and dried in vacuo. Yield: 3.8 g (93%). IR (KBr, $cm^{-1}$): 3650 vs, 1770 s, 1690 vs, 1635 w, 1610 s, 1590 s, 1560 m, 1270 s, 1210 s, 845 m, 730 m, 720 s, 700 s. $^1$H NMR (DMSO-$d_6$): $\delta$ 9.75 (s, 1H, $H_9$), 6.97 (d, 2H, $H_{8,10}$, $^3J$ = 8.67), 6.82 (d, 2H; $H_{7,11}$, $^3J$ = 8.67), 6.59 (s, 2H, $H_{2,3}$), 5.22 (s, 2H, $H_{1,4}$), 3.03 (s, 2H, $H_{5,6}$). $^{13}$C NMR ($CDCl_3$): $\delta$ 175.4 ($C_{7,8}$), 136.7 ($C_{12}$), 131.8 ($C_{2,3}$), 129.2 ($C_{10,14}$), 128.8 ($C_9$), 126.6 ($C_{11,13}$), 81.5 ($C_{1,4}$), 47.6 ($C_{5,6}$). Elemental analysis: Calcd for $C_{14}H_{11}NO_4$ ($M_w$ = 257.24): C, 65.37; H, 4.31; N, 5.44. Found: C, 65.08; H, 4.46; N, 5.36.

**4-(*N*,*N*-Dimethyl)maleic Monoanilide (VIII).** Maleic anhydride (1.5 g, 0.15 mol) was dissolved in diethyl ether, and 4-amino-*N*,*N*-dimethylaniline (20.4 g, 0.15 mol) was added. The solution was refluxed for 16 h, and the precipitate was filtered off, washed with cold diethyl ether, and dried in vacuo. Yield: 32.9 g (93%). IR (KBr, $cm^{-1}$): 3280 m, 3190 m, 3080 bs, 3050 w, 1705 vs, 1695 vs, 1635 s, 1610 s, 1540 w, 1520 bm, 1425 w, 1400 s, 1370 s, 1230 m, 845 vs, 805 vs, 640 s. $^1$H NMR ($CDCl_3$): $\delta$ 7.11 (m, AA′BB′, 2 H, $J_1$ = 9.1), 6.79 (s, 1 H, C=C*H*), 6.74 (m, AA′BB′, 2 H, $J_1$ = 9.1), 2.95 (s, 6 H, $CH_3$). $^{13}$C NMR ($CDCl_3$): $\delta$ 170.5 (*C*O), 150.5 $C_{ipso}$, 134.3 (*C*=C), 127.5 $C_{ipso}$, 119.7, 112.8, 40.7 (N−*C*$H_3$). Elemental analysis: Calcd for $C_{12}H_{14}N_2O_3$ ($M_w$ = 234.25): C, 61.53; H, 6.02; N, 11.96. Found: C, 61.54; H, 5.92; N, 11.90.

**4-(*N*,*N*-Dimethylaminophenyl)maleimide (IX).** Sodium acetate anhydrous (5.64 g, 70 mmol) was added to a solution of 4-(*N*,*N*-dimethyl)maleic monoanilide (32.9 g, 141 mmol) in acetic anhydride. The reaction mixture was stirred at 130 °C for 18 h and poured onto ice. The solution was adjusted to pH 8 using sodium bicarbonate. The oily precipitate was extracted with dichloromethane, and the solvent was evaporated under reduced pressure. The residue was Soxhlet-extracted for 60 h using cyclohexane. Finally cyclohexane was evaporated under reduced pressure. Yield: 22.1 g (73%). IR (KBr, $cm^{-1}$): 3380 bs, 3090 s, 3060 s, 3020 w, 2890 m, 1755 vs, 1670 s, 1580 s, 1230 m, 1220 m, 805 m, 790 s, 730 vs. $^1$H NMR ($CDCl_3$): $\delta$ 7.14 (d, 2H, $H_{1,2}$), 6.78 (m, 4H, $H_{3,4,5,6}$), 2.98 (s, 6H, $H_{7,8}$). $^{13}$C NMR ($CDCl_3$): $\delta$ 176.2 ($C_{1,4}$), 150.7 ($C_8$), 136.8 ($C_{2,3}$), 127.4 ($C_{6,10}$), 120.3 ($C_5$), 112.6 ($C_{7,9}$), 40.6 ($C_{11,12}$).

***exo*,*exo*-*N*-(4-(*N*′,*N*′-Dimethylaminophenyl)-7-oxanorborn-2-ene-5,6-dicarbimide (X).** 4-(*N*,*N*-Dimethylphenyl)-maleimide (4.0 g, 18.6 mmol) dissolved in diethyl ether and furan (2.7 mL, 37 mmol) were placed in an autoclave and held at 90 °C for 18 h. The reaction mixture was cooled to 0 °C, and a precipitate formed. It was filtered off, washed with cold diethyl ether, and dried under reduced pressure. Yield: 3.1 g (80%). IR (KBr, $cm^{-1}$): 3010 s, 2900 s, 1770 m, 1700 s, 1610 m, 1590 m, 1450 m, 1390 m, 1240 m, 825 w, 710 s, 700 s. $^1$H NMR ($CDCl_3$): $\delta$ 7.10 (td, 2H, $H_{7,10}$, $^3J$ = 9.03, $^4J$ = 3.0, $^5J$ = 2.2), 6.75 (td, 2H, $H_{8,9}$, $^3J$ = 9.0, $^4J$ = 3.0, $^5J$ = 2.25), 6.55 (s, 2H, $H_{2,3,}$ $J$ = 2), 5.38 (t, 2H, $H_{1,4}$ $J$ = 1.14, $J$ = 0.75), 2.98 (s, 8H, $H_{5,6,11,12}$). $^{13}$C NMR ($CDCl_3$): $\delta$ 170.4 ($C_{7,8}$), 150.4 ($C_{12}$), 134.3 ($C_{2,3}$), 127.5 ($C_{10,14}$), 127.2 ($C_9$); 119.7 ($C_{5,6}$), 112.7 ($C_{11,13}$), 40.7 ($C_{1,4}$), 40.6 ($C_{15,16}$). Elemental analysis: Calcd for $C_{16}H_{16}N_2O_3$ ($M_w$ = 284.31): C, 67.59; H, 5.67; N, 9.85. Found: C, 67.38; H, 5.46; N, 9.75.

**Norborn-2-ene-5-ylmethylhydroxysiloxyl-*β*-cyclodextrin (XI).** *β*-Cyclodextrin (3.0 g, 2.64 mmol) was dissolved in 100 mL of dry pyridine and cooled to −15 °C. Bicyclo[2.2.1]-hept-2-ene-5-methyldichlorosilane (1.0 mL, 5.56 mmol, $\rho$ = 1.1513) was added. The reaction temperature was allowed to rise to room temperature within 1 h, and stirring was continued overnight. Pyridine was evaporated under reduced pressure until a white residue remained. The white residue was thoroughly washed with acetone, recrystallized from DMF/acetone, and dried in vacuo. Yield: 2.2 g (65%). $^1$H NMR (DMF-$d_6$): $\delta$ (selected): 6.0 (b, C=C). $^{13}$C NMR (DMF-$d_6$): $\delta$ (selected): 138.5 ($C_{3endo}$), 135.4 ($C_{3exo}$), 135.3 ($C_{2endo}$), 134.1 ($C_{2exo}$). Elemental analysis: Calcd for $CyH_{80}SiO_{35}$ ($M_w$ = 1268.7 g/mol): C, 47.31; H, 6.31. Found: C, 46.79; H, 6.69.

***endo/exo*-7-Oxabicyclo[2.2.1]norborn-2-ene-5-carboxylic Acid Chloride (XII).** Freshly distilled furan (80 mL, 1.1 mol) and acrylic acid chloride (30 mL, 0.37 mol) were stirred at room temperature for 3 days. Excess furan and unreacted acrylic acid chloride were removed under reduced pressure (0.2 Torr, −20 °C). Yield: 23.1 g (39.4%). NMR studies revealed 23% *exo*- and 77% *endo*-**XII**. $^1$H NMR ($CDCl_3$): $\delta$ 6.31 (dd, $H_{3exo}$, $^3J$ = 6.0, $^3J$ = 1.5), 6.27 (dd, $H_{3endo}$, $^3J$ = 6.0, $^3J$ = 1.5), 6.19 (dd, $H_{2exo}$, $^3J$ = 6.0, $^3J$ = 1.5), 6.17 (dd, $H_{2endo}$, $^3J$ = 6.0, $^3J$ = 1.5), 5.11 (s, $H_{4exo}$), 5.10 (s, $H_{4endo}$), 4.90 (d, $H_1$, $^3J$ = 4.5, $^3J$ = 5.3), 3.42 (m, $H_{5exo}$, $^3J$ = 3.75, $^3J$ = 4.45), 2.74 (q, $H_{5endo}$, $J$ = 4.14), 2.24 (m, $H_{6exo/exo}$ $^3J$ = 3.7, $^3J$ = 4.9), 1.99 (td, $H_{6exo/endo}$, $^3J$ = 4.14, $^3J$ = 4.5, $^2J$ = 11.67), 1.92 (m, $H_{6endo/exo}$, $^3J$ = 4.14, $^2$J, = 4,53 Hz), 1.46 (td, $H_{6endo/endo}$, $^3J$ = 3.57, $^3J$ = 4.89). $^{13}$C NMR ($CDCl_3$): $\delta$ 174.1 ($C_7$), 138.0 ($C_{3endo}$), 137.0 ($C_{3exo}$), 133.9 ($C_{2endo}$), 132.8 ($C_{2exo}$), 80.7 ($C_{4endo}$), 79.5 ($C_{4exo}$), 79.2 ($C_{1endo}$), 78.1 ($C_{1exo}$), 55.3 ($C_5$), 29.9 ($C_{6endo}$), 29.1 ($C_{6exo}$).

***endo/exo*-7-Oxanorborn-2-ene-5-carboxyl-carboxyl-*β*-cyclodextrin (XIII)**. *β*-Cyclodextrin (2 g, 1.76 mmol) was

dried in refluxing toluene in a Dean−Stark apparatus and subsequently dissolved in 35 mL of dry pyridine and cooled to −40 °C. 7-Oxanorborn-2-enecarboxylic chloride (1.7 g, 11.2 mmol) was added. The reaction temperature was allowed to rise to room temperature, and stirring was continued overnight. Pyridine was removed under reduced pressure at 40 °C until a light yellow residue remained. Acetone was added, and the precipitate was filtered off, washed with acetone, and dried in vacuo. 7-Oxanorborn-2-ene-5-carboxyl-$\beta$-cyclodextrin was recrystallized from DMF/acetone. Yield: 1.75 g (79%). IR (KBr, $cm^{-1}$): 3300 bs $\nu$(OH), 2927 s, 1729 m $\nu$(C=O), 1659 s, 1541 m, 1490 m, 1156 m, 1097 m $\nu$(C−O), 1004 s, 945 m, 937 m, 864 m. $^1$H NMR (DMSO-$d_6$): $\delta$ 6.39 (s, $H_{2,3}$), 4.98 (s, $H_4$), 4.86 (s, 7H, $H_{1'}$), 4.38 (s, broad, $H_{6'OH}$), 4.11 (s, broad, $H_{4'}$), 3.64 (m, $H_{6'}$), 3.37 (m, $H_{4',2'}$) 2.44 (s, broad, $H_5$), 1.91 (s, broad, $H_{6exo}$), 1.44 (s, broad, $H_{6endo}$). $^{13}$C NMR (DMSO-$d_6$): $\delta$ 173.1($C_7$), 145.7 ($C_{3endo}$), 145.2 ($C_{3exo}$), 144.4 ($C_{3endo}$), 143.1 ($C_{3exo}$), 101.9 ($C_{1'}$), 81.5 ($C_{4'}$), 80.4 ($C_4$), 77.2 ($C_1$), 72.9 ($C_{3'}$), 72.0 ($C_5'$), 68.9 ($C_{2'}$), 63.8 ($C_{6'+NBE}$), 59.8 ($C_{6'}$), 42.1 ($C_5$), 28.6 ($C_6$).

***exo,exo-N*-(4-Trimethylsilyloxyphenyl)-7-oxanorborn-2-ene-5,6-dicarbimide (XIV).** *exo,exo-N*-(4-Hydroxyphenyl)-7-oxanorborn-2-ene-5,6-dicarbimide (4.3 g, 16.7 mmol) was suspended in THF and cooled to −50 °C. *n*-Butyllithium (2 M in hexane, 8.5 mL, 17.0 mmol) was added, and the mixture was warmed to 0 °C. After 5 min, the suspension was again cooled to −50 °C, and chlorotrimethylsilane (2.5 mL, 20 mmol) was added. The reaction mixture was allowed to warm to room temperature and was stirred for a further 2 h. The solvent was evaporated, and the residue was dissolved in diethyl ether. Flash chromatography through silica G-60 (220−400 mesh, 4 × 20 cm) allowed the separation of the product. Recrystallization from diethyl ether yielded 2.7 g (49%). IR (KBr): 1706 vs, 1310 vs, 1386s, 1252 s, 1180 s, 1145m, 1060 m, 1013 s, 912s, 845m, 803 m, 755 m, 705 m, 695 m, 648 s. $^1$H NMR ($CDCl_3$): $\delta$ 7.15−6.80 (m, AA′BB′, 4 H, $J$ = 12), 6.55 (s, 2 H), 5.37 (s, 2 H), 2.94 (s, 2 H), 0.26 (s, 9 H, $OSi(CH_3)_3$), $^{13}$C NMR ($CDCl_3$): $\delta$ 175.9, 136.8, 127.9, 125.1, 120.7, 116.2, 81.5, 47.6, 0.4. Elemental analysis: Calcd for $C_{17}H_{19}NO_4Si$ ($M_w$ = 329.428): C, 61.98; H, 5.81; N, 4.25. Found: C, 62.9; H, 5.95; N, 4.09.

**Polymerizations. Preparation of Linear Polymers.** $Cl_2Ru(PCy_3)_2(CHC_6H_5)$-based polymerizations using 0.1 g of the corresponding monomer were carried out at 60 °C in dry 1,2-dichloroethane or DMF and terminated by adding 1-hexene. Polymers were precipitated with methanol or *n*-pentane and dried in vacuo.

**Poly-IV.** Yield: 93%. $M_w$ = 3500, PDI = 1.40. $^1$H NMR ($CDCl_3$): $\delta$ 7.4−7.2 (m, 5 H, phenyl), 6.04 (bs, $HC{=}CH_{trans'}$), 5.8 (bs, $HC{=}CH_{cis}$), 5.14 (s, $C_{allyl,\ cis}$), 4.62 (s, $C_{allyl,\ trans}$), 3.35 (s, 2 H, COC*H*). $^{13}$C NMR ($CDCl_3$): $\delta$ 174.3 (CO), 131.4 ($C_m$), 129.3 ($C{=}C_{trans}$), 128.8 ($C_p$), 126.5 ($C{=}C_{cis}$), 126.3 ($C_o$), 81.2 (*C*CO), 52.1 ($C_{allyl}$). Trans:cis ≈ 5:2.

**Poly-VII.** Yield: 27%. $M_w$ = 1700, PDI = 1.18. $^1$H NMR ($CDCl_3$): $\delta$ 9.78 (s, 1 H, O*H*), 7.1 (bs, 2 H, $H_o$), 6.8 (s, 2 H, $H_m$), 6.00 ($HC{=}CH_{trans}$), 5.77 ($HC{=}CH_{cis}$), 5.04 (s, $CH_{allyl,\ cis}$), 4.60 ($CH_{allyl,\ trans}$), 3.50 (NCOC*H*). $^{13}$C NMR ($CDCl_3$): $\delta$ 174.2 (CO), 157.3 ($C_p$), 131.4 ($C{=}C_{trans}$), 128.4 ($C_m$), 123.1 ($C{=}C_{cis}$), 115.3 ($C_o$), 79.9 ($C_{allyl}$), 52.2 (NCO*C*). Trans:cis ≈ 3:1

**Poly-X.** Yield: 77%. $M_w$ = 4400, PDI = 1.35. $^1$H NMR ($CDCl_3$): $\delta$ 7.05 (b, 2H), 6.7 (b, 2H), 6.13 (s, $CH{=}CH,_{trans}$), 5.85 (s, $CH{=}CH,_{cis}$), 5.15 ($H_{\beta,cis}$), 4.55 (m, $H_{\beta,trans}$), 3.42 ($H_\gamma$), 2.80 (s, 6 H, methyl). $^{13}$C NMR ($CDCl_3$): $\delta$ 175.8 (CO), 151.0, 127.8, 120.4 ($C{=}C_{trans}$), 112.6 ($C{=}C_{cis}$), 81.7 ($H_\gamma$), 78.15 ($H_{\beta,\ trans}$), 68.3 ($H_{\beta,\ cis}$), 40.7 (methyl). Trans:cis ≈ 5:2.

**Poly-XIV.** Yield: 89%. $M_w$ = 2600, PDI = 1.07. $^1$H NMR ($CDCl_3$): $\delta$ 7.1 (bs, 2 H), 6.9 (bs, 2 H), 6.1 (bs, $C{=}C{-}H_{trans}$), 5.8 (s, $C{=}C{-}H_{cis}$), 5.2 ($H_{allyl-cis}$), 4.6 ($H_{ally-trans}$), 3.4 (COC*H*), 0.24 (s, 9 H, $OSi(CH_3)_3$). $^{13}$C NMR ($CDCl_3$): $\delta$ 175.0 (*C*O), 155.5 ($C_{ipso}$), 130.8 ($C{=}C_{trans}$), 127.5, 124.7 ($C{=}C_{cis}$), 120.5, 81.0 (*C*CO), 52.1 ($C_{allyl}$), 0.20 ($OSi(CH_3)_3$). Trans:cis ≈ 4:1.

**Pretreatment of HPLC Glass Columns.** Borosilicate glass columns (50 × 3 mm, 150 × 3 mm, 250 × 3 mm, i.d., Omnifit, Cambridge, England) and 100 × 3 mm Chrompack were etched with saturated ethanolic KOH overnight. After repeated washing with water, columns were dried under air at 90 °C for 2 h. Silanization was performed at 60 °C overnight using a mixture of pyridine/toluene and bicyclo[2.2.1]hept-2-ene-5-trichlorosilane (molar ratio 3:2:1). Glass columns were washed consecutively with acetone, water, ethanol, and dry ethanol and dried under reduced pressure at ambient temperature. All monoliths were prepared by standard Schlenk techniques as follows: A HPLC column was placed in a test tube of similar diameter and cooled to the corresponding polymerization temperature ($T_p$, Table 1). Two different solutions (A, B) were prepared and cooled to $T_p$. Solution A consisted of the monomer, the cross-linker, and the macroporogen; solution B consisted of the microporogen and the initiator. Solutions A and B were merged and mixed for a few seconds. The polymerization mixture was then filled into the test tube in a way that the borosilicate column was completely filled and covered (Figure 4). The column was then kept at $T_p$ for 30 min, and polymerization was allowed to complete at room temperature overnight. The test tube was broken, and the polymeric material at the outside of the HPLC column was removed. The column was provided with end fittings and attached to a HPLC system. The same microporogenic solvent used for solution B was pumped through the column at a flow rate of 0.1 mL/min for several hours to remove all soluble compounds still present in the polymer rod after polymerization. Morphologies were investigated by electron microscope (ELMI). Graphs of back-pressure vs flow were recorded using water as the mobile phase.

**Polymerization Characteristics**. A mixture of DMN-H6, 2-propanol, toluene, and initiator as used for the synthesis of monolith **14** (Table 1) was polymerized at $T$ = 0 °C. Polymer samples were withdrawn every 30 s and simultaneously terminated by adding these samples to a 1: 1 mixture of 1-hexene and acetonitrile. Finally, samples were filtered and characterized by GPC.

**Functionalized Monoliths.** Functionalized monoliths were prepared identically to nonfunctionalized ones. For functionalized monoliths 5D−5I solution A consisted of NBE, DMN-H6, and 2-propanol (0.25/0.25/0.4). Solution B consisted of toluene and initiator **1** (0.1/0.01). For monoliths 7J and 7K solution A consisted of NBE, DMN-H6, and 2-propanol (0.3/0.3/0.3); solution B consisted of toluene and initiator **1** (0.1/0.01). One hour after polymerization was started, test tubes were broken and columns were provided with end fittings. Columns were rinsed with the appropriate solvent before passing 1 mL of a 10 wt % solution of the corresponding functional monomer in the same solvent through the column. Dichloromethane was used as solvent for monomers **I**, **II**, **III**, **IV**, and **X** (monoliths 4D, 4E, 4F, and 4H); DMF was used for **VII**, **XI**, and **XIII** (monoliths 4G, 6J, and 6K). Columns were sealed at both ends, and polymerization was allowed to complete overnight at 60 °C. Finally, columns were consecutively washed with the same solvent used for derivatization and acetonitrile prior to use.

**Determination of the Optimum Polymerization Time.** In three different experiments, toluene was passed through three identical monoliths (type 5) 30, 60, and 120 min after initiation. Toluene fractions were dried under reduced pressure, and the obtained residues were investigated for their monomer content.

**Acknowledgment.** The authors thank Dr. G. Stingl, Institute of Mineralogy and Petrography, University of Innsbruck, for the recording of all ELMI pictures. Financial support was provided by the Austrian National Science Foundation (FWF, Vienna, Austria), Project P12963-GEN, and the "Jubiläumsfonds der Österreichischen Nationalbank", Project 7489.

## References and Notes

(1) Buchmeiser, M. R. *J. Chromatogr. A*, in press.

(2) Huber, C. G.; Kleindienst, G.; Bonn, G. K. *Chromatographia* **1997**, *44*, 438.

(3) Huber, C. K.; Oefner, P. J.; Bonn, G. K. *Anal. Biochem.* **1993**, *212*, 351.
(4) Huber, C. G.; Oefner, P. J.; Preuss, E.; Bonn, G. K. *Nucl. Acid Res.* **1993**, *21*, 1061.
(5) Tennikova, T. B.; Bleha, M.; Svec, F.; Almazova, T. V.; Belenkii, B. G. *J. Chromatogr.* **1991**, *555*, 97.
(6) Kiyohara, S.; Kim, M.; Toida, Y.; Sugita, K.; Sugo, T. *J. Chromatogr. A* **1997**, *758*, 209.
(7) Sunaga, K.; Kim, M.; Saito, K.; Sugita, K.; Sugo, T. *Chem. Mater.* **1999**, *11*, 1986.
(8) Gerstner, J. A.; Hamilton, R.; Cramer, S. M. *J. Chromatogr.* **1992**, *596*, 173.
(9) Kennedy, J. F.; Paterson, M. *Polym. Int.* **1993**, *32*, 71.
(10) Yang, Y.; Velayudhan, A.; Ladisch, C. M.; Ladisch, M. R. *J. Chromatogr.* **1992**, *598*, 169.
(11) Hansen, L. C.; Sievers, R. E. *J. Chromatogr.* **1974**, *99*, 123.
(12) Hosoya, K.; Ohta, H.; Yoshizoka, K.; Kimatas, K.; Ikegami, T.; Tanaka, N. *J. Chromatogr. A* **1999**, *853*, 11.
(13) Maruska, A.; Ericson, C.; Végvári, A.; Hjertén, S. *J. Chromatogr. A* **1999**, *837*, 25.
(14) Gusev, I.; Huang, X.; Horváth, C. *J. Chromatogr. A* **1999**, *855*, 273.
(15) Tang, Q.; Xin, B.; Lee, M. L. *J. Chromatogr. A* **1999**, *837*, 35.
(16) Asiaie, R.; Huang, X.; Farnan, D.; Horváth, C. *J. Chromatogr. A* **1998**, *806*, 251.
(17) Peters, E. C.; Petro, M.; Svec, F.; Fréchet, J. M. J. *Anal. Chem.* **1997**, *69*, 3646.
(18) Peters, E. C.; Petro, M.; Svec, F.; Fréchet, J. M. J. *Anal. Chem.* **1998**, *70*, 2288.
(19) Xie, S.; Svec, F.; Fréchet, J. M. J. *Chem. Mater.* **1998**, *10*, 4072.
(20) Rodrigues, A. E. *J. Chromatogr. A* **1997**, *699*, 47.
(21) Xu, Y.; Liapis, A. I. *J. Chromatogr. A* **1996**, *724*, 13.
(22) Hjertén, S.; Liao, J.-L.; Zhang, R. *J. Chromatogr.* **1989**, *473*, 273.
(23) Hjertén, S.; Li, Y.-M.; Liao, J.-L.; Mohammad, J.; Nakazato, K.; Pettersson, G. *Nature* **1992**, *356*, 810.
(24) Peters, E. C.; Svec, F.; Fréchet, J. M. J. *Adv. Mater.* **1999**, *11*, 1169.
(25) Svec, F.; Fréchet, J. M. J. *Science* **1996**, *273*, 205.
(26) Viklund, C.; Svec, F.; Fréchet, J. M. J.; Irgum, K. *Chem. Mater.* **1996**, *8*, 744.
(27) Viklund, C.; Pontén, E.; Glad, B.; Irgum, K.; Hörstedt, P.; Svec, F. *Chem. Mater.* **1997**, *9*, 463.
(28) Sykora, D.; Svec, F.; Fréchet, J. M. J. *J. Chromatogr. A* **1999**, *852*, 297.
(29) Wang, Q. C.; Svec, F.; Fréchet, J. M. J. *Anal. Chem.* **1993**, *65*, 2243.
(30) Svec, F.; Fréchet, J. M. J. *Macromolecules* **1995**, *28*, 7580.
(31) Xie, S.; Svec, F.; Fréchet, J. M. J. *J. Polym. Sci., Part A: Polym. Chem.* **1997**, *35*, 1013.
(32) Peters, E. C.; Svec, F.; Fréchet, J. M. J. *Chem. Mater.* **1997**, *9*, 1898.
(33) Podgornik, A.; Barut, M.; Jancar, J.; Strancar, A. *J. Chromatogr. A* **1999**, *848*, 51.
(34) Svec, F.; Fréchet, J. M. J. *J. Chromatogr. A* **1995**, *702*, 89.
(35) Tennikov, M. B.; Gazdina, N. V.; Tennikova, T. B.; Svec, F. *J. Chromatogr. A* **1998**, *798*, 55.
(36) Wang, Q. C.; Svec, F.; Fréchet, J. M. J. *Anal. Chem.* **1995**, *67*, 670.
(37) Buchmeiser, M. R.; Atzl, N.; Bonn, G. K. *J. Am. Chem. Soc.* **1997**, *119*, 9166.
(38) Buchmeiser, M. R.; Tessadri, R.; Seeber, G.; Bonn, G. K. *Anal. Chem.* **1998**, *70*, 2130.
(39) Buchmeiser, M. R.; Mupa, M.; Seeber, G.; Bonn, G. K. *Chem. Mater.* **1999**, *11*, 1533.
(40) Buchmeiser, M. R.; Sinner, F.; Mupa, M.; Wurst, K. *Macromolecules* **2000**, *33*, 32.
(41) Sinner, F.; Buchmeiser, M. R.; Tessadri, R.; Mupa, M.; Wurst, K.; Bonn, G. K. *J. Am. Chem. Soc.* **1998**, *120*, 2790.
(42) Buchmeiser, M. R.; Wurst, K. *J. Am. Chem. Soc.* **1999**, *121*, 11101.
(43) Sinner, F.; Buchmeiser, M. R. *Angew. Chem., Int. Ed. Engl.* **2000**, *39*, 1433.
(44) Fisher, R. A.; Grubbs, R. H. *Makromol. Chem., Macromol. Symp.* **1992**, *63*, 271.
(45) Davidson, T. A.; Wagner, K. B. *J. Mol. Catal. A: Chem.* **1998**, *133*, 67.
(46) Davidson, T. A.; Wagener, K. B.; Priddy, D. B. *Macromolecules* **1996**, *29*, 786.
(47) Cooper, A. I.; Holmes, A. B. *Adv. Mater.* **1999**, *11*, 1270.
(48) István, H.; Kornél, M. *Angew. Chem.* **1978**, *9*, 954.
(49) Svec, F.; Fréchet, J. M. J. *Chem. Mater.* **1995**, *7*, 707.
(50) Takata, T.; Endo, T. *Prog. Polym. Sci.* **1993**, *18*, 839.
(51) Penczek, S.; Kubisa, P.; Szymanski, R. *Makromol. Chem., Rapid Commun.* **1991**, *12*, 77.
(52) Johnson, A. F.; Mohsin, M. A.; Meszena, Z. G.; Graves-Morris, P. *J. Macromol. Sci., Rev. Macromol. Chem. Phys.* **1999**, *C39*, 527.
(53) Szwarc, M. *J. Polym. Sci., Part A: Polym. Chem.* **1998**, *36*, ix.
(54) Webster, O. W. *Science* **1991**, *251*, 887.
(55) Peters, E. C.; Svec, F.; Fréchet, J. M. J.; Viklund, C.; Irgum, K. *Macromolecules* **1999**, *32*, 6377.
(56) Szwarc, M. *Makromol. Chem., Rapid Commun.* **1992**, *13*, 141.
(57) Matyjaszewski, K. *Macromolecules* **1993**, *26*, 1787.
(58) Ulman, M.; Grubbs, R. H. *J. Org. Chem.* **1999**, *64*, 7202.
(59) Diels, O.; Alder, K. *Chem. Ber.* **1929**, *62*, 554.
(60) Alder, K.; Backendorf, K. H. *Ann. Chem.* **1938**, *535*, 101.
(61) Lu, S.-Y.; Quayle, P.; Heatly, F.; Booth, C.; Yeates, S. G.; Padget, J. C. *Eur. Polym. J.* **1993**, *29*, 269.
(62) Benedicto, A. D.; Novak, B. M.; Grubbs, R. H. *Macromolecules* **1992**, *25*, 5893.
(63) Anderson, W. K.; Milowsky, A. S. *J. Org. Chem.* **1985**, *50*, 5423.
(64) Stille, J. K.; Frey, D. A. *J. Am. Chem. Soc.* **1959**, *81*, 4273.
(65) Schwab, P.; Grubbs, R. H.; Ziller, J. W. *J. Am. Chem. Soc.* **1996**, *118*, 100.
(66) Halász, I.; Martin, K. *Angew. Chem.* **1978**, *90*, 954.

MA000322N